NPS-69-81-001A

NAVAL POSTGRADUATE SCHOOL

Monterey, California

EFFECTS OF CAVITATION ON UNDERWATER

SHOCK LOADING - PLANE PROBLEM, FINAL REPORT

R. E. NEWTON
March 1981

Final Report for Period
October 1979 - September 1980

Approved for Public Release; Distribution Unlimited

Prepared for:

Defense Nuclear Agency
Washington, D. C. 20305

NAVAL POSTGRADUATE SCHOOL
Monterey, California

Rear Admiral J. J. Ekelund
Superintendent

D. A. Schrady
Acting Provost

The work reported herein was supported by the Defense Nuclear Agency under the FY 1980 Program, Subtask Y99QAXSF501.

UNCLASSIFIED

SECURITY CLASSIFICATION OF THIS PAGE (When Data Entered)

REPORT DOCUMENTATION PAGE	READ INSTRUCTIONS BEFORE COMPLETING FORM
1. REPORT NUMBER: NPS-69-81-001A.	2. GOVT ACCESSION NO. / 3. RECIPIENT'S CATALOG NUMBER
4. TITLE (and Subtitle): EFFECTS OF CAVITATION ON UNDERWATER SHOCK LOADING - PLANE PROBLEM, FINAL REPORT	5. TYPE OF REPORT & PERIOD COVERED: Final, October 79-September 80
	6. PERFORMING ORG. REPORT NUMBER
7. AUTHOR(s): R. E. Newton	8. CONTRACT OR GRANT NUMBER(s): MIPR 80-509
9. PERFORMING ORGANIZATION NAME AND ADDRESS: Naval Postgraduate School, Monterey, CA 93940	10. PROGRAM ELEMENT, PROJECT, TASK AREA & WORK UNIT NUMBERS: Y99QAXSF501, Work Unit 16
11. CONTROLLING OFFICE NAME AND ADDRESS: Defense Nuclear Agency SPSS, Washington, C.D. 20305	12. REPORT DATE: March 1981
	13. NUMBER OF PAGES: 33
14. MONITORING AGENCY NAME & ADDRESS(If different from Controlling Office)	15. SECURITY CLASS. (of this report): Unclassified
	15a. DECLASSIFICATION/DOWNGRADING SCHEDULE

16. DISTRIBUTION STATEMENT (of this Report)

Approved for Public Release; Distribution Unlimited

17. DISTRIBUTION STATEMENT (of the abstract entered in Block 20, if different from Report)

18. SUPPLEMENTARY NOTES

19. KEY WORDS (Continue on reverse side if necessary and identify by block number)

Underwater shock, cavitation, finite elements

20. ABSTRACT (Continue on reverse side if necessary and identify by block number)

Final results of an investigation of the effects of response-induced cavitation on underwater shock loading are reported. Data were obtained by finite element modeling of a submerged sandwich shell and a surrounding plane fluid region. Representative curves are presented showing shell bending stress, hoop compressive stress and contents acceleration as functions of time. It is concluded that, for the range of parameters considered, cavitation does not increase the severity of loading on structure or equipment.

DD FORM 1 JAN 73 1473 EDITION OF 1 NOV 68 IS OBSOLETE
S/N 0102-014-6601

UNCLASSIFIED
SECURITY CLASSIFICATION OF THIS PAGE (When Data Entered)

20. (continued)

Application of the finite element modeling technique is recommended for investigation of bulk cavitation and its effects on structural loading.

TABLE OF CONTENTS

EFFECTS OF CAVITATION ON UNDERWATER SHOCK LOADING - PLANE PROBLEM, FINAL REPORT

1. Introduction

Earlier phases of this investigation were described in a series of reports. Problems of dependent variable selection were considered in Ref. 1. The viability and utility of a displacement potential were demonstrated by solving a representative one-dimensional problem and obtaining results in good agreement with those obtained earlier by Bleich and Sandler and reported in Ref. 2. An unsuccessful effort to use ADINA for applications with axisymmetric geometry was described in Ref. 3.

Development of a finite element FORTRAN IV program (DPLPOT) to trace, for plane regions, the propagation of underwater shock, including effects of response-induced cavitation, was described in Ref. 4. A mesh generator (MGNEW) was also developed for these applications. Reference 5 describes the construction of a computer program (STRUK5) to determine the transient response of a submerged cylindric structure. Early results obtained with the concurrent use of STRUK5, or its successor, STRUK6, and the fluid program DPLPOT were reported in Refs. 6 and 7.

The present report summarizes results for the plane problem. Data presented are representative of findings from over 500 separate computer runs. For the range of parameters considered, conclusions are given concerning the effects of cavitation on the severity of structural loading.

2. Scope of Investigation

2.1 Fluid Parameters

Properties of the fluid are representative of seawater with density = 1024 kg/m^3 and acoustic velocity c = 1500 m/s. The fluid region is rectangular (see Fig. 1). Hydrostatic pressure P_h is uniform because a gravity induced gradient would violate the assumed symmetry relative to y = 0.

Incident shock waves have plane fronts (x = const.) with step rise of height P_s, followed by exponential decay with characteristic length L. To simulate the effect of surface cutoff, a limited number of runs were made using box waves of length L.

The piecewise linearity of the fluid constitutive law (Ref. 1) reduces the number of different combinations of P_h, P_s, and L that need to be investigated. Specifically, if L and P_s/P_h are fixed, response variables such as shell bending moments, stresses, and accelerations vary in direct proportion to the shock pressure P_s.

The shell radius used throughout is R = 5 m. The decay lengths of incident shock waves were 7.5 m, 15 m, and 30 m, corresponding to decay times of 5 ms, 10 ms, and 20 ms. As reported previously, when cavitation occurs it begins at least one decay length in front of the structure (x > R + L in Fig. 1). Since the boundary conditions at entry, top, and exit faces are valid only if the adjacent fluid is uncavitated, the required region size is problem dependent. Except in very short runs used to look at fine details of the early

behavior, the exit face was located at x = -13.5 m. Position of the top face ranged from y = 22 m to y = 72 m. For the entry face, the normal range was from x = 36 m to x = 108 m.

A useful program feature that allows determination of cavitation effects by direct comparison is an "ON-OFF" switch for cavitation. In the "OFF" mode, the fluid pressure is the same linear function of condensation for negative pressure as it is for positive pressure and no cavitation occurs.

2.2 Structure Parameters

As noted above, a shell radius R = 5 m was used throughout. The sandwich shell, made from steel with modulus of elasticity E = 210 GPa and density ρ_s = 7830 kg/m^3, consisted of inner and outer shells, each 25 mm thick, joined by a massless core 291 mm deep.* The core is assumed to make no contribution to circumferential or flexural rigidity, but to provide a rigid shear connection between inner and outer shells.

The addition of a single internal mass ("contents" mass), elastically coupled to the shell rigid body mode (n = 1), was described in Ref. 6. A subsequent refinement has added viscous damping in parallel with the elastic suspension of the contents mass. Because the contents mass has its magnitude adjusted to make the assembly neutrally buoyant, the only additional parameters introduced by its inclusion are the (fixed base)

---

*This unlikely core depth corresponds to $(r_g/R)^2 = .001$, where r_g is the section radius of gyration.

frequency f_c and critical damping fraction ζ of the suspension. For most of the cases investigated the choices f_c = 10 Hz and ζ = .10 have been made.

2.3 Spatial and Temporal Subdivision

Appropriate choices of mesh subdivision and the step size used in time integration have been the subject of extensive investigation. It is clear that finer grids are capable of producing improved accuracy. If both structure and fluid were governed by elliptic partial differential equations, the ideal compromise would provide a fine grid at the structure and in the adjacent fluid. In the remainder of the fluid, the element size would increase with distance from the structure. Because the fluid behavior is governed by a hyperbolic partial differential equation, such a graded mesh is not satisfactory.

The dilemma posed is as follows. Satisfactory simulation of wave propagation in the fluid requires a substantially uniform subdivision throughout. The choice made for the fluid determines the number of interface fluid nodes and compatibility requirements at the interface dictate an equal number of structural nodes.* Thus, the structural subdivision is fixed by the choice made for the fluid. Best accuracy for time integration in the fluid requires the largest time step compatible with stability, whereas the accuracy attained for the structure improves as the time step size is decreased.

---

*This constraint results from the kind of structural model used here and is not a necessary condition for all fluid-structure interactions.

In the face of these conflicting requirements, the compromise adopted was based on the following choices. For full field problems, the number of fluid nodes and the number of fluid elements was approximately 3000. The time step was chosen to be approximately one-fifth the period of the highest frequency structural mode. Mesh data and time steps are summarized in Table 1 for the three decay lengths investigated.

Table 1. Mesh Data

	Decay length, L		
	7.5 m	15 m	30 m
Number of fluid nodes	3558	3088	3004
Number of fluid elements	3392	2950	2880
Element side, largest	.69 m	1.11 m	1.84 m
Element side, smallest	.49 m	.79 m	1.31 m
Structural degrees of freedom	64	40	24
Time step	.031 ms	.05 ms	.10 ms

3. Response as a Function of Time

3.1 Parameters for Chosen Cases

In the following sections, time histories for shell bending stress, hoop compressive stress, and contents acceleration are presented for three selected encounters. Parameters used, together with Figure numbers for the relevant curves, are given in Table 2.

Table 2. Parameters for Time Histories

L	p_h	p_s	θ	Figure Numbers
7.5 m	.4 MPa	12 MPa	0°	2, 5, 8
15 m	.4 MPa	12 MPa	180°	3, 6, 9
30 m	.2 MPa	12 MPa	0°	4, 7, 10

Time is measured from the instant of first contact between shock front and shell. This occurs when the shock front is at $x = R = 5$ m.

3.2 Shell Bending Stress

At the location of first contact ($\theta = 0$, Fig. 1), the bending stress rises rapidly, usually attaining its first maximum within 5 ms. A representative set of curves showing bending stress as a function of time is given in Fig. 2. Positive bending stress corresponds to compressive stress on the external surface of the hull. Results are for decay length $L = 7.5$ m at $\theta = 0$. The curve labeled ON reveals that cavitation causes a higher maximum bending stress at $T = 68$ ms

than at T = 1 ms. The curve labeled OFF (cavitation suppressed) shows the same early peak, but no comparable late-time maximum. A parallel set of results for $\theta = 180°$ and L = 15 m is given in Fig. 3. A third set, for $\theta = 0$ and L = 30 m, is given in Fig. 4.

In order to assess the effects of cavitation on stress, it is necessary to know where and when cavities appear. In all cases based on realistic parameters, the first cavity appears at a distance of about one decay length L in front of the hull after at least one decay time (T = L/c)*. This cavity and the effects of its closure do not perceptibly influence shell bending stresses. At a later time, there may be cavitation at and near the hull. The late time bending stress extrema in Figs. 2, 3, and 4 all coincide approximately with closures of such hull cavities.

3.3 Hoop Compressive Stress

Superposed on the circumferential compressive stress resulting from external hydrostatic pressure are very high transient stresses induced by the shock loading. Representing compressive stresses as positive, dynamic hoop stresses as a function of time are given in Figs. 5, 6, and 7 for the same cases as in Figs. 2, 3, and 4.

In all cases, it will be observed that the first direct stress extremum occurs between T = 7 ms and T = 11 ms. This

---

*For the box wave, cavitation first occurs about one-half box length in front of the hull and at an earlier time.

extremum is not affected by cavitation. At late times, the effects of cavitation are discernible, but the corresponding extrema are no greater than 15% of the initial one.

3.4 Contents Acceleration

The acceleration of the contents mass is an indication of the severity of the shock motion transmitted to equipment. Time history of the contents acceleration is presented in Figs. 8, 9, and 10 for the three cases previously considered. The first extremum occurs before T = 12 ms. The second extremum is usually of approximately equal magnitude, but opposite sign. The effects of cavitation upon the largest (absolute) accelerations are insignificant.

4. Structural Importance of Cavitation

4.1 Bending Stress

The hull bending stresses shown in Figs. 2, 3, and 4 all show late time extrema associated with the closures of cavities at the hull. In Fig. 3, this peak is larger and of greater duration than the early one. It is believed that the hull cavitation encountered is induced by the large amplitude shell motion that occurs in phase opposition to the response motion of the contents mass. This behavior was illustrated in Figs. 1 and 2 of Ref. 6 and is shown again here as Fig. 11. A more realistic and elaborate model of the contents would introduce many additional degrees of freedom with a diversity of individual frequencies. The accompanying shell motion might reasonably be expected to have smaller amplitude and be less regular.

An indication of the dependence of the hull cavitation effects on the contents model is shown in Fig. 12. Here, the solid curve is the same as in Fig. 3 and the dotted curve shows what happens to shell bending stress when the contents suspension frequency is reduced from 10 Hz to 5 Hz. This change eliminates the hull cavitation and, thus, the late time stress peak. There is a striking similarity between the dotted curve of Fig. 12 and that of Fig. 3. In the latter case, cavitation was artificially suppressed.

For the parameters of Fig. 2, a change of suspension frequency from 10 Hz to 5 Hz will again suppress hull cavitation and eliminate the late time stress peak. The effect

is shown in Fig. 13.

In consideration of these results, it is concluded that the late time bending stress peaks of Figs. 2, 3, and 4 are spurious effects of the oversimplified contents model. It follows that cavitation does not increase the extreme values of bending stress.

4.2 Hoop Compressive Stress

The results presented in Figs. 5, 6, and 7 show that early time peaks in dynamic hoop compressive stress are unaffected by cavitation. Although cavitation does seem to make late time peaks higher, the latter are so small in comparison with the early peaks that the cavitation effects do not affect structural survival.

Attention is directed to the very large magnitudes of peak values of hoop compressive stress compared with those associated with shell bending. It is clear that the largest resultant stresses occur at early times and that late time bending stress peaks will produce much smaller resultants than at early times. This lends additional support to the proposition that cavitation does not increase the likelihood of hull collapse.

4.3 Internal Equipment

The contents mass of the structural model may be considered to represent a lumping of internal structure and equipment. It is a very crude model, but the contents accelerations presented in Figs. 8, 9, and 10 show that

extreme values are not significantly affected by cavitation. Although a more elaborate model would be required to predict with confidence the accelerations of particular equipment items, the conclusion that cavitation does not significantly affect peak structural accelerations is unlikely to be reversed by using a more complex model.

4.4 Effects of Surface Cutoff

At moderate submergence depths with large horizontal standoff, the incident shock pulse is abruptly truncated by a negative pressure wave reflected from the free surface. As was mentioned above, a limited number of runs were made using an incident box wave to simulate this effect. Details of response to this altered wave-form are omitted here because the behaviors found are qualitatively identical with those reported in Section 3.

5. Conclusions

For the response-induced cavitation that has been the subject of this investigation, none of the results obtained indicates that cavitation increases the likelihood of structural or equipment failure. There is a remaining possibility that the large deflections accompanying inelastic shell response might induce close-in cavitation whose collapse would produce higher extreme structural loadings. Study of inelastic response and the accompanying geometric nonlinearity is beyond the scope of this investigation.

6. Recommendation

The investigation which is completed with this report has dealt with response-induced cavitation. The parameters have been chosen to represent attacks on submerged submarines and bulk cavitation induced by the free surface has been excluded.

There is abundant evidence, both experimental and analytic, that bulk cavitation and the subsequent cavity collapse may produce, for surface ships, significant increases in the severity of shock loadings. It is recommended that the finite element technique based on a potential function be extended to the important class of problems featuring water borne shock loads in the presence of bulk cavitation.

7. References

1. Newton, R. E., "Effects of Cavitation on Underwater Shock Loading - Part 1," NPS69-78-013, Naval Postgraduate School, Monterey, CA, July 1978.

2. Bleich, H. H., and I. S. Sandler, "Interaction between Structures and Bilinear Fluids," International Journal of Solids and Structures, Vol. 6, p. 617, 1970.

3. Newton, R. E., "Effects of Cavitation on Underwater Shock Loading - Axisymmetric Geometry," NPS69-78-017PR, Naval Postgraduate School, Monterey, CA, November 1978.

4. Newton, R. E., "Effects of Cavitation on Underwater Shock Loading - Plane Problem, Part 1," NPS69-79-007PR, Naval Postgraduate School, Monterey, CA, July 1979.

5. Waller, J. T., "Dynamic Structural Model of a Submerged Ring," M.Sc. Thesis, Naval Postgraduate School, Monterey, CA, September 1979.

6. Newton, R. E., "Effects of Cavitation on Underwater Shock Loading - Plane Problem, Part 2," NPS69-80-001, Naval Postgraduate School, Monterey, CA, April 1980.

7. Newton, R. E., "Finite Element Study of Shock Induced Cavitation," Preprint 80-110, ASCE Spring Convention, April 1980.

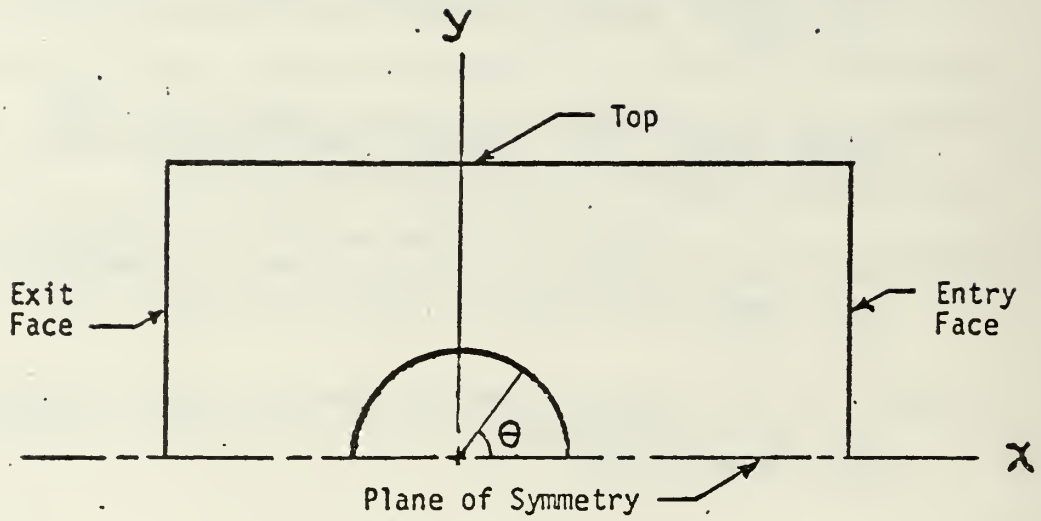

Fig. 1. Geometry of plane fluid region.

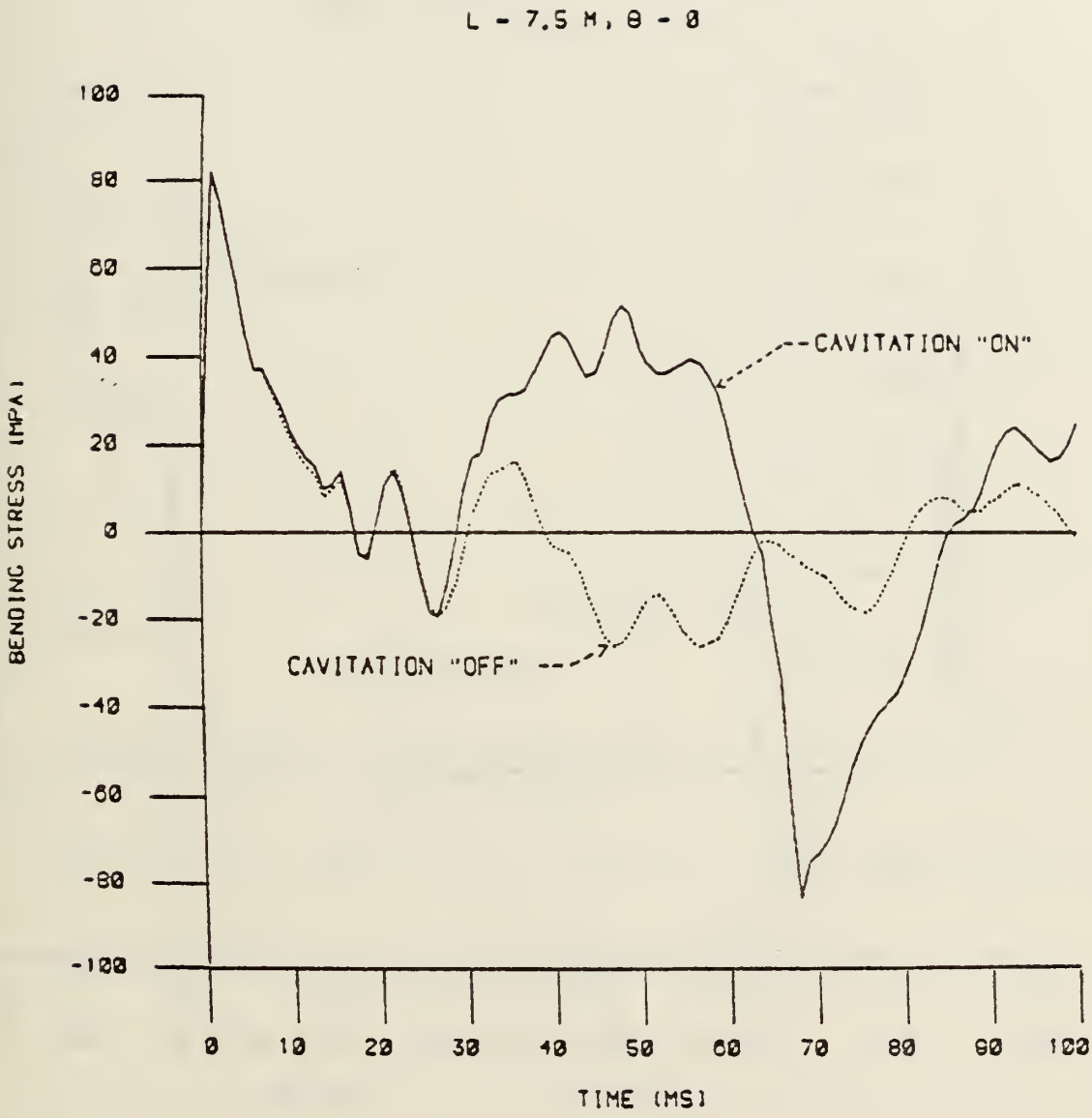

Fig. 2. Shell bending stress vs. time, L = 7.5 m.

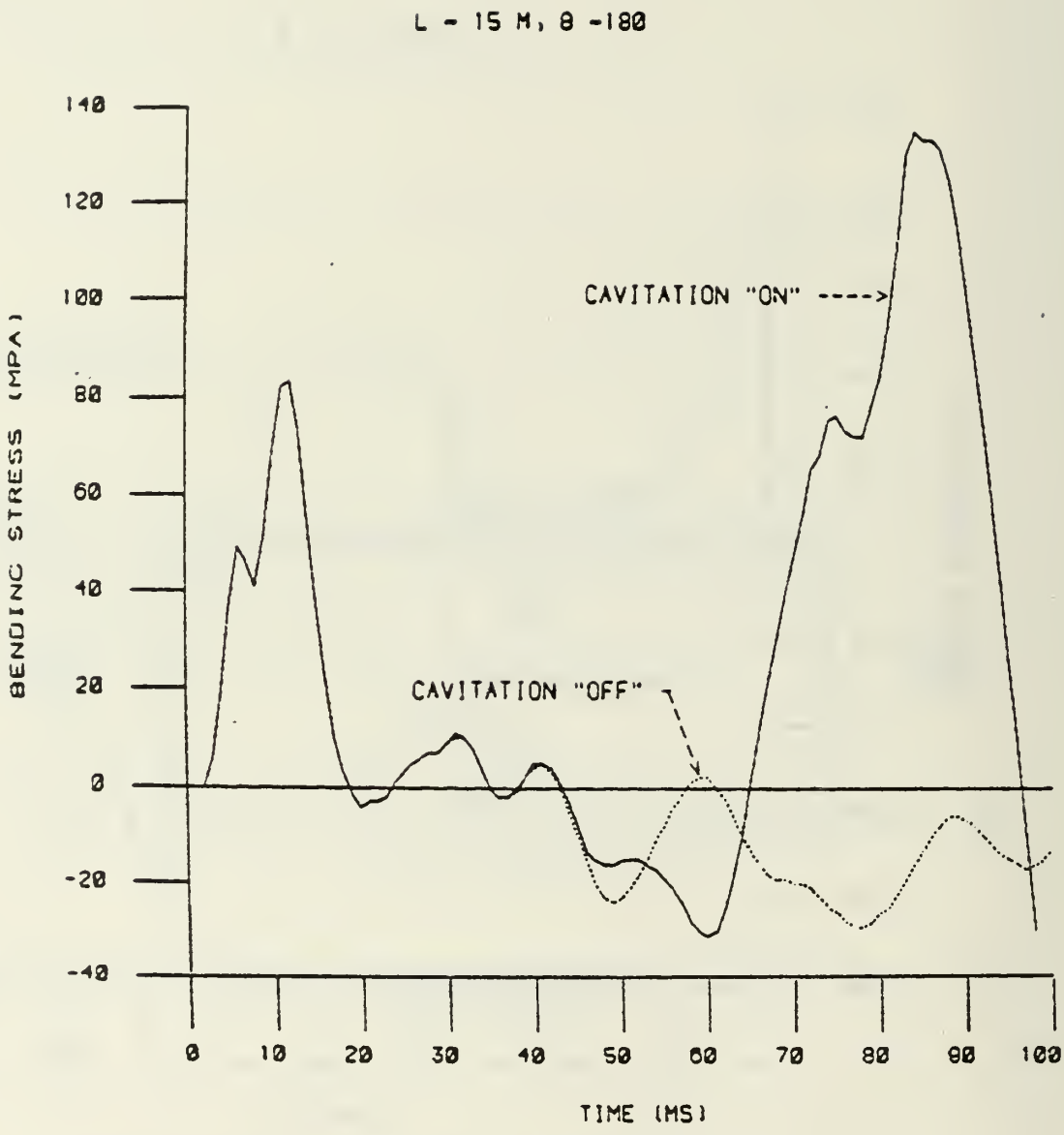

Fig. 3. Shell bending stress vs. time, L = 15 m.

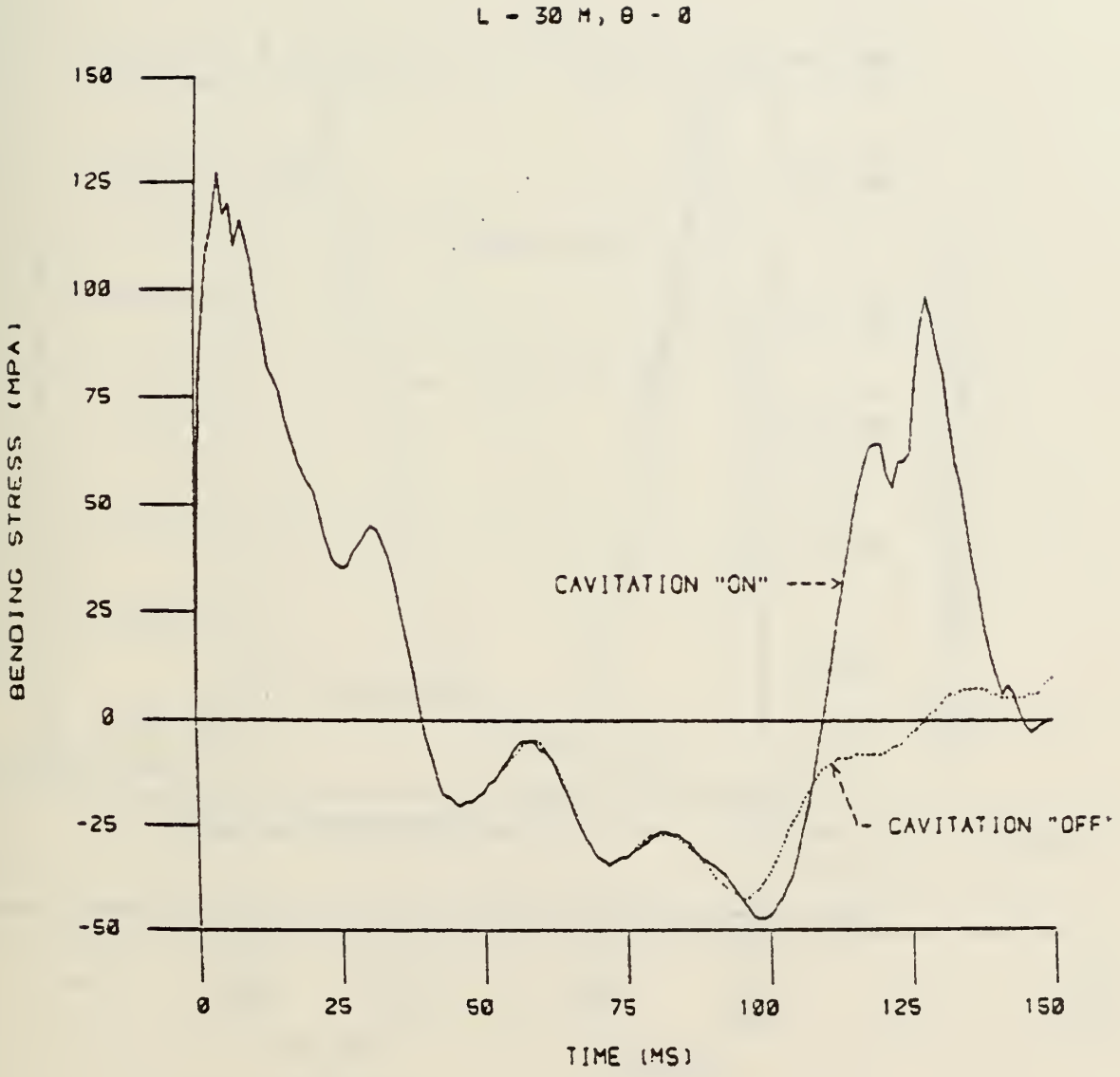

Fig. 4. Shell bending stress vs. time, L = 30 m.

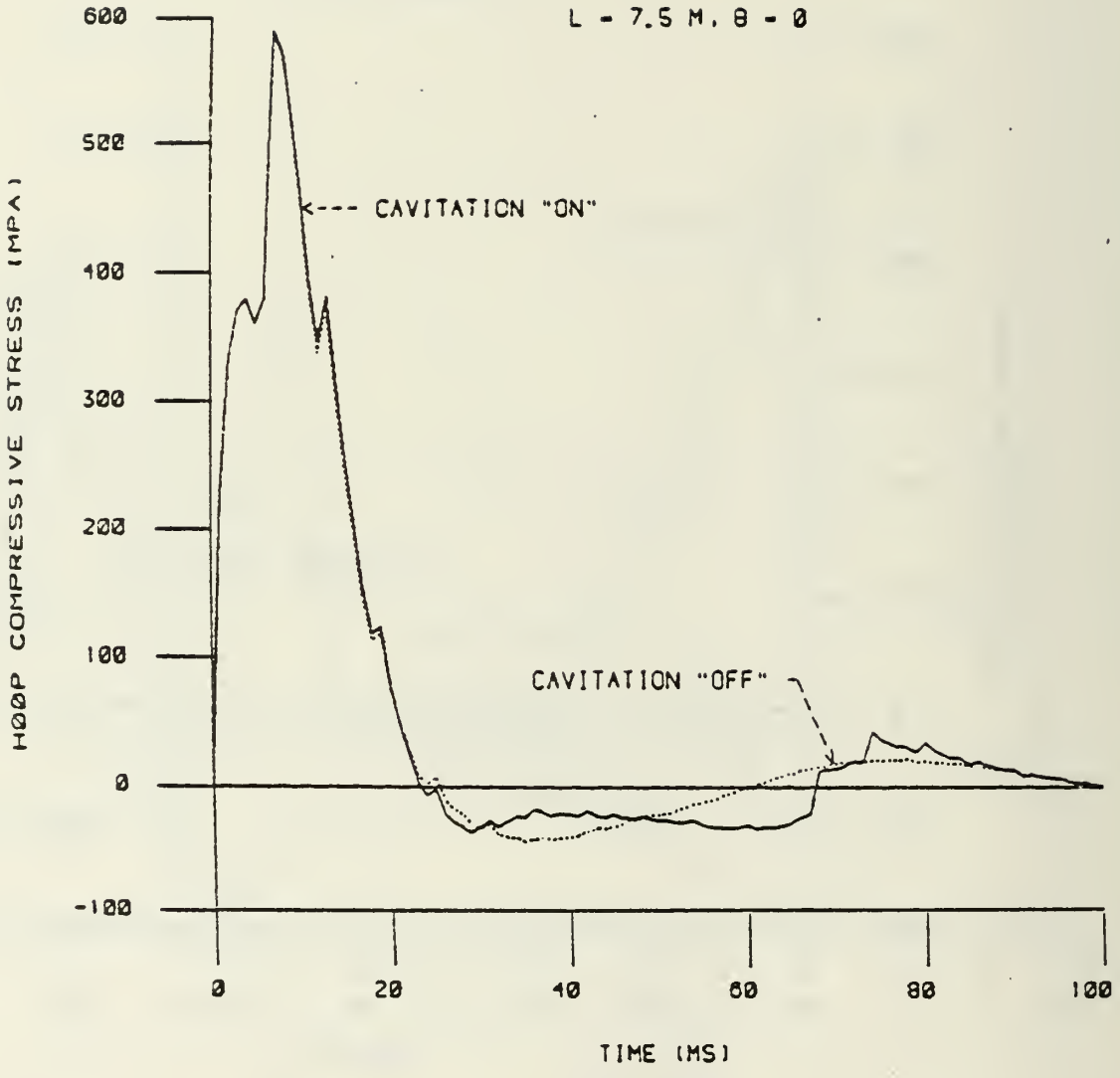

Fig. 5. Hoop compressive stress vs. time, L = 7.5 m.

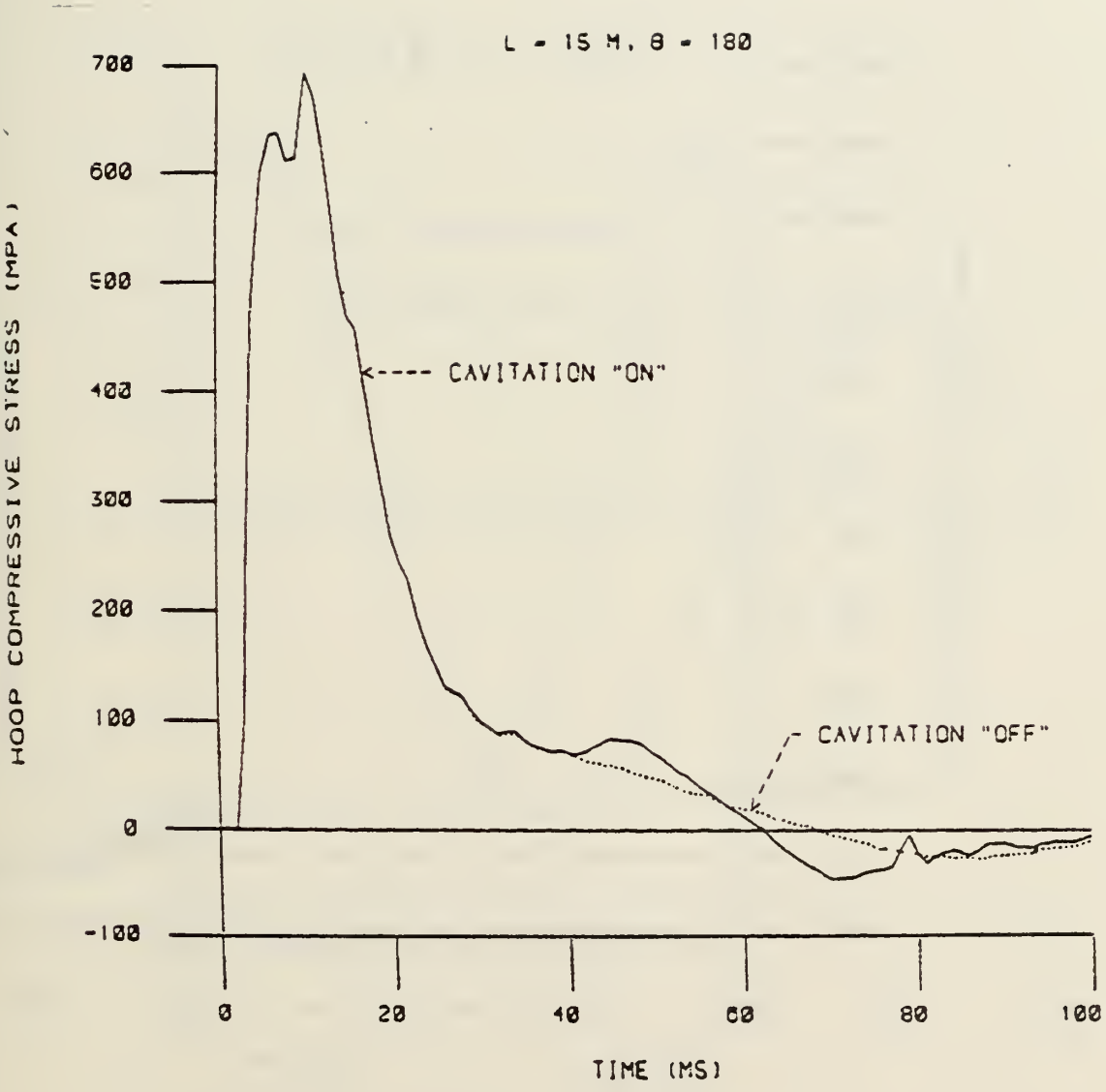

Fig. 6. Hoop compressive stress vs. time, L = 15 m.

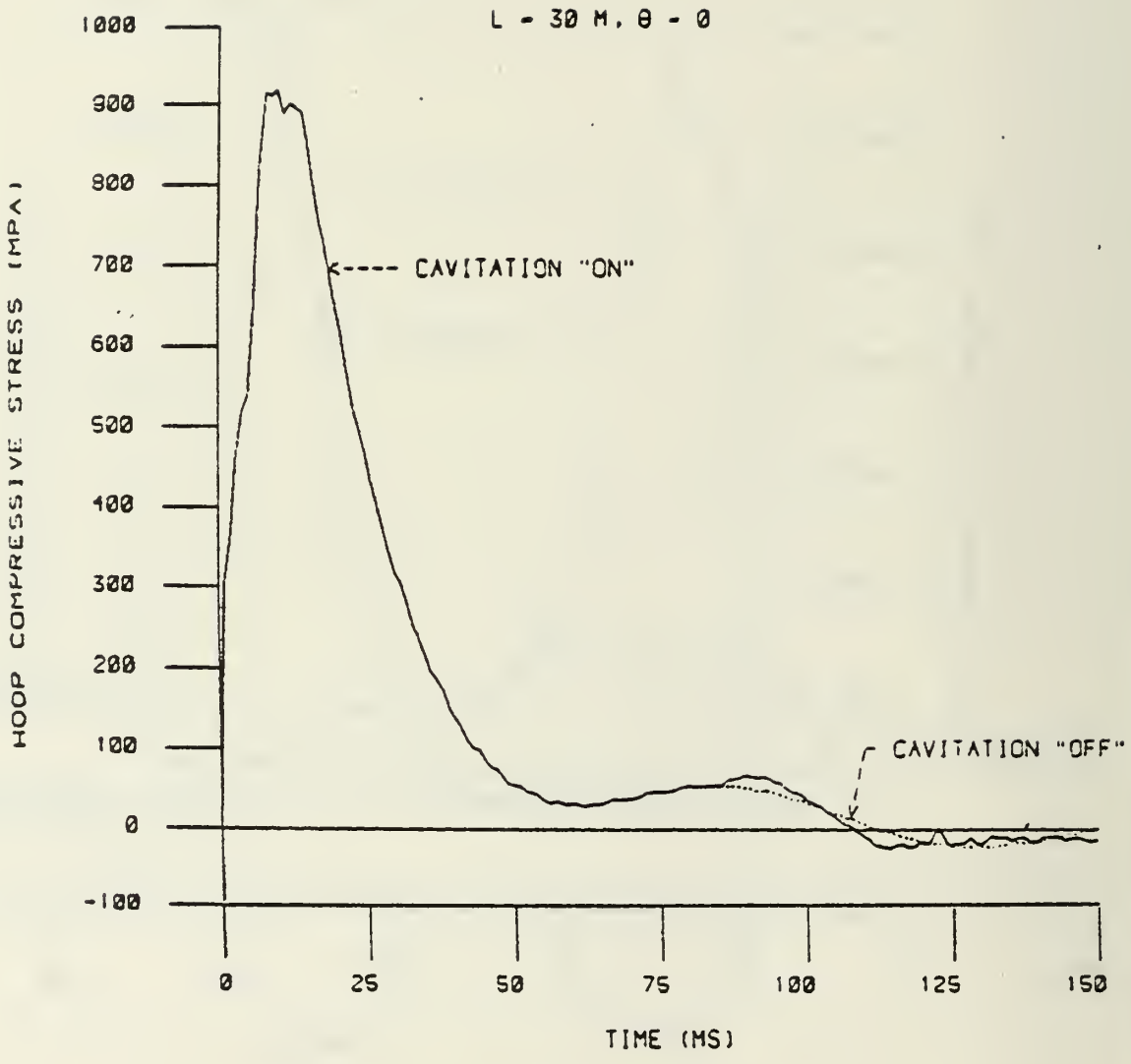

Fig. 7. Hoop compressive stress vs. time, L = 30 m.

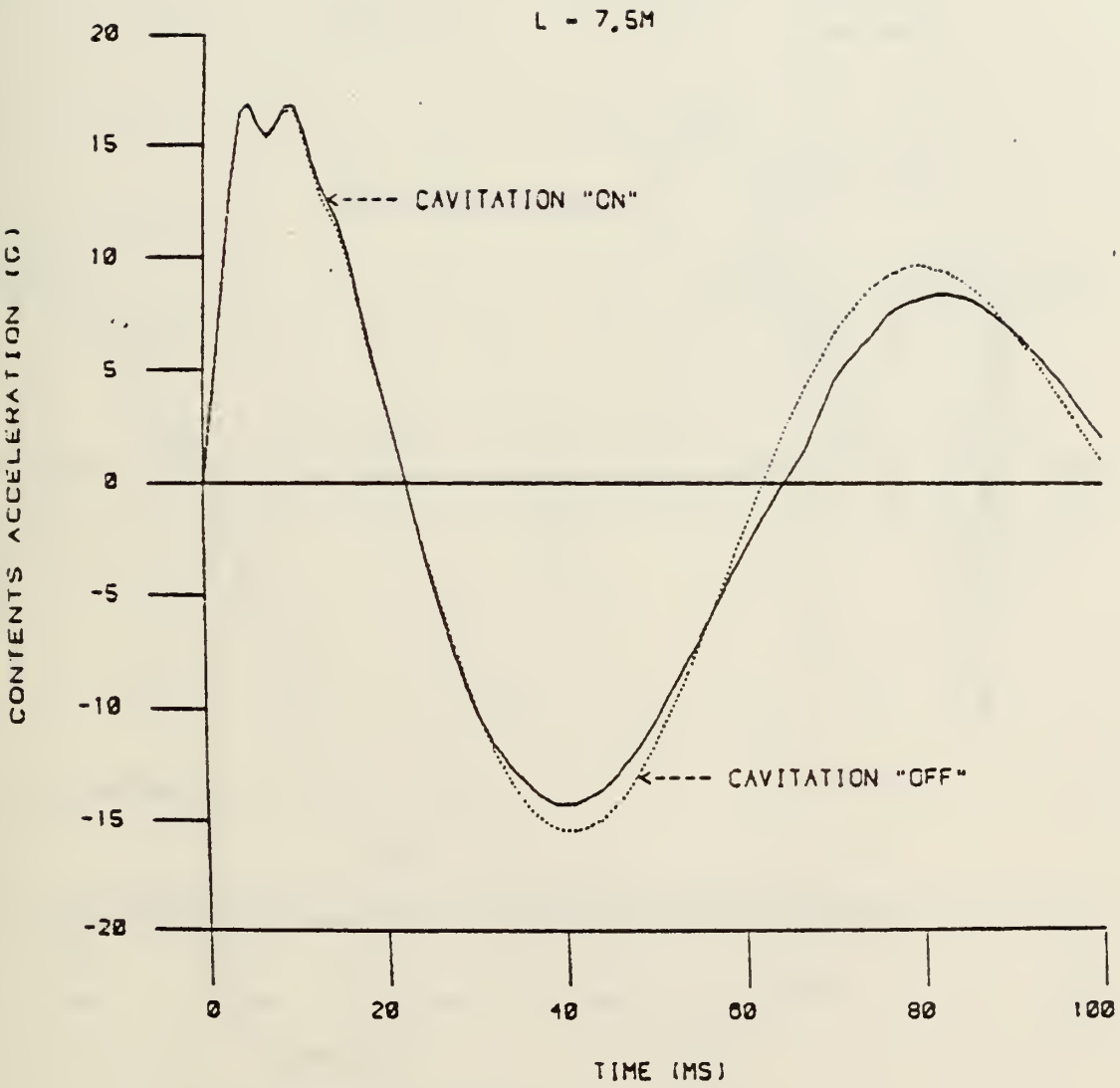

Fig. 8. Contents acceleration vs. time, L = 7.5 m.

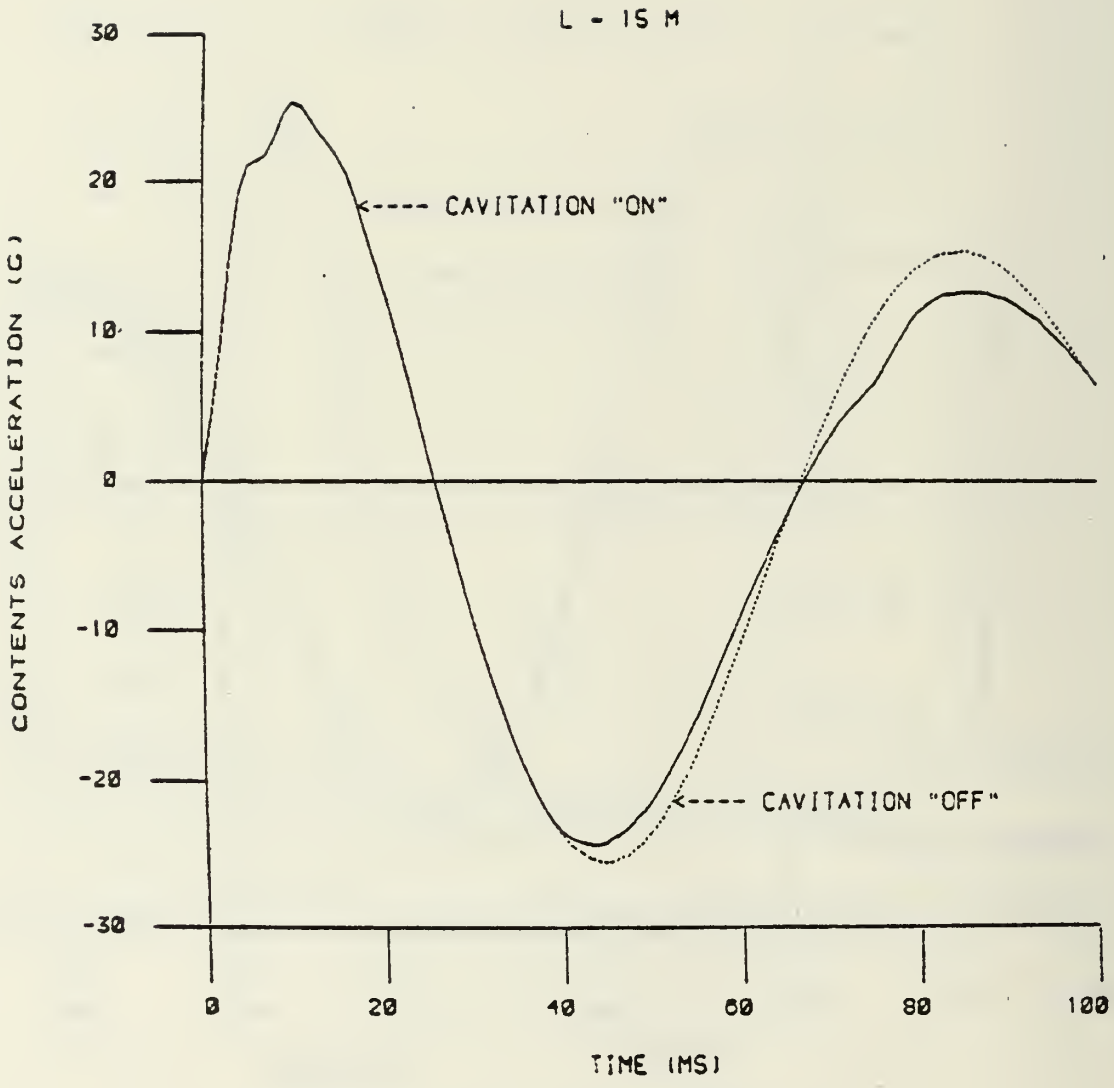

Fig. 9. Contents acceleration vs. time, L = 15 m.

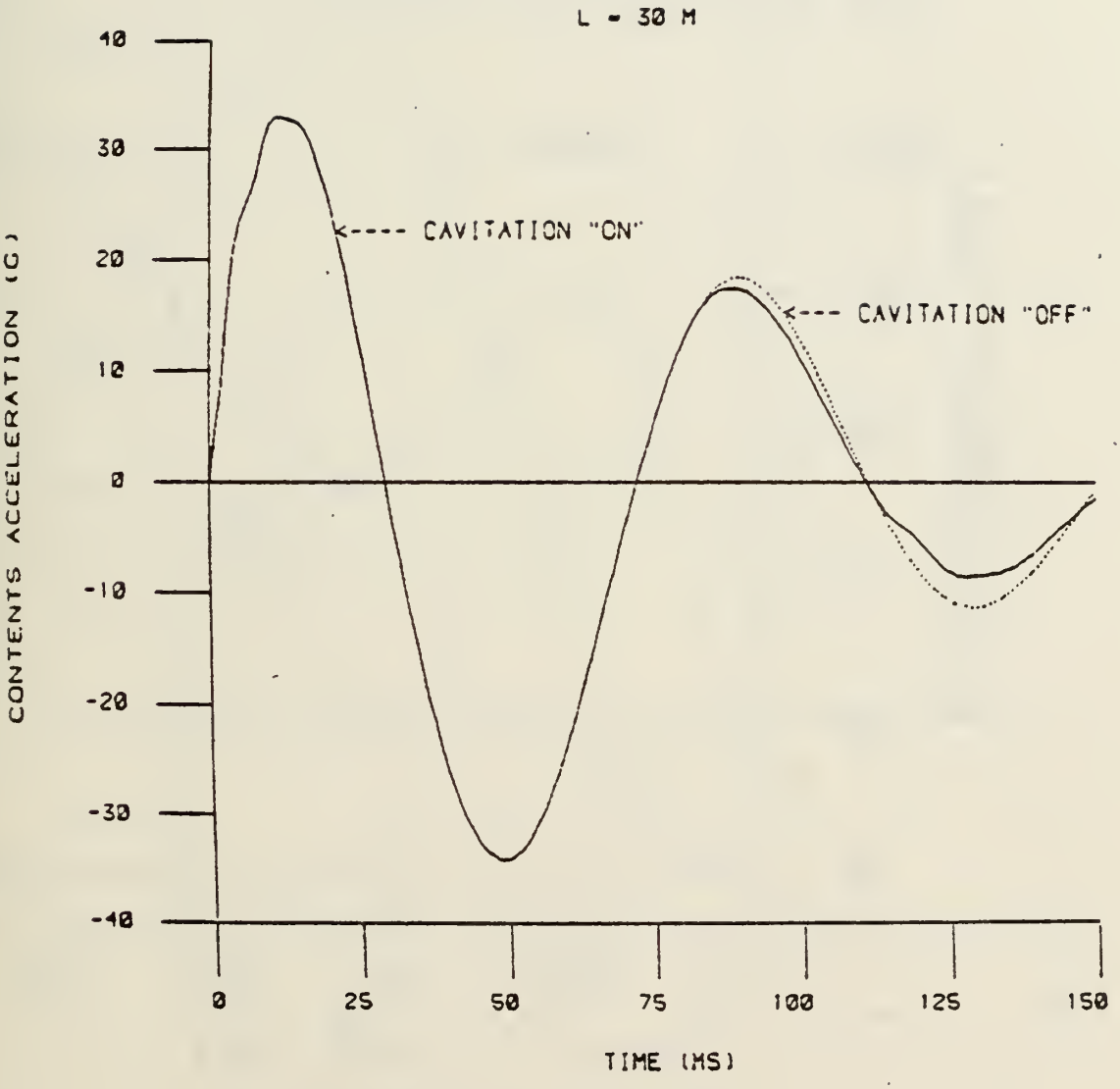

Fig. 10. Contents acceleration vs. time, L = 30 m.

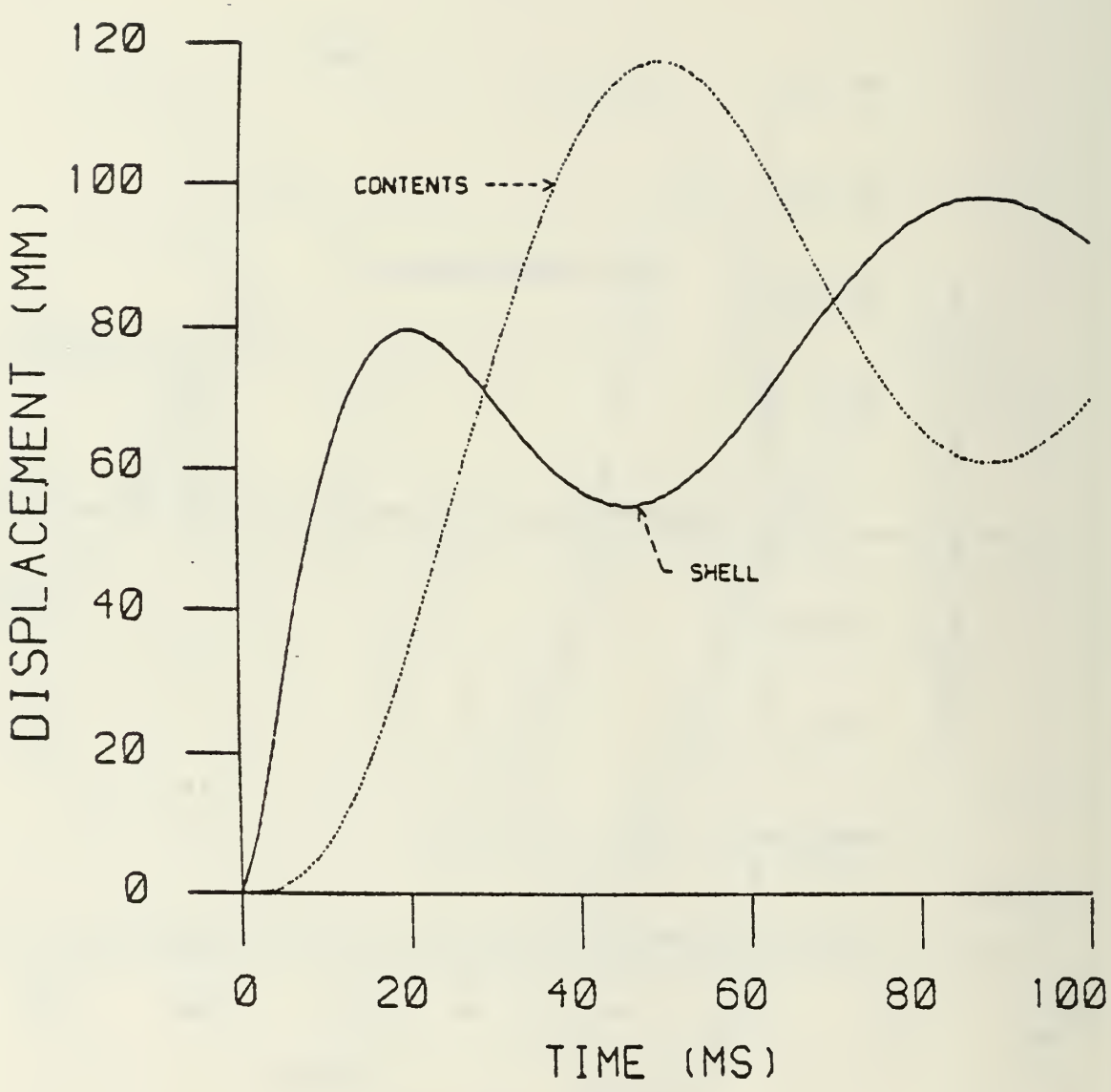

Fig. 11. Shell and contents displacement vs. time.

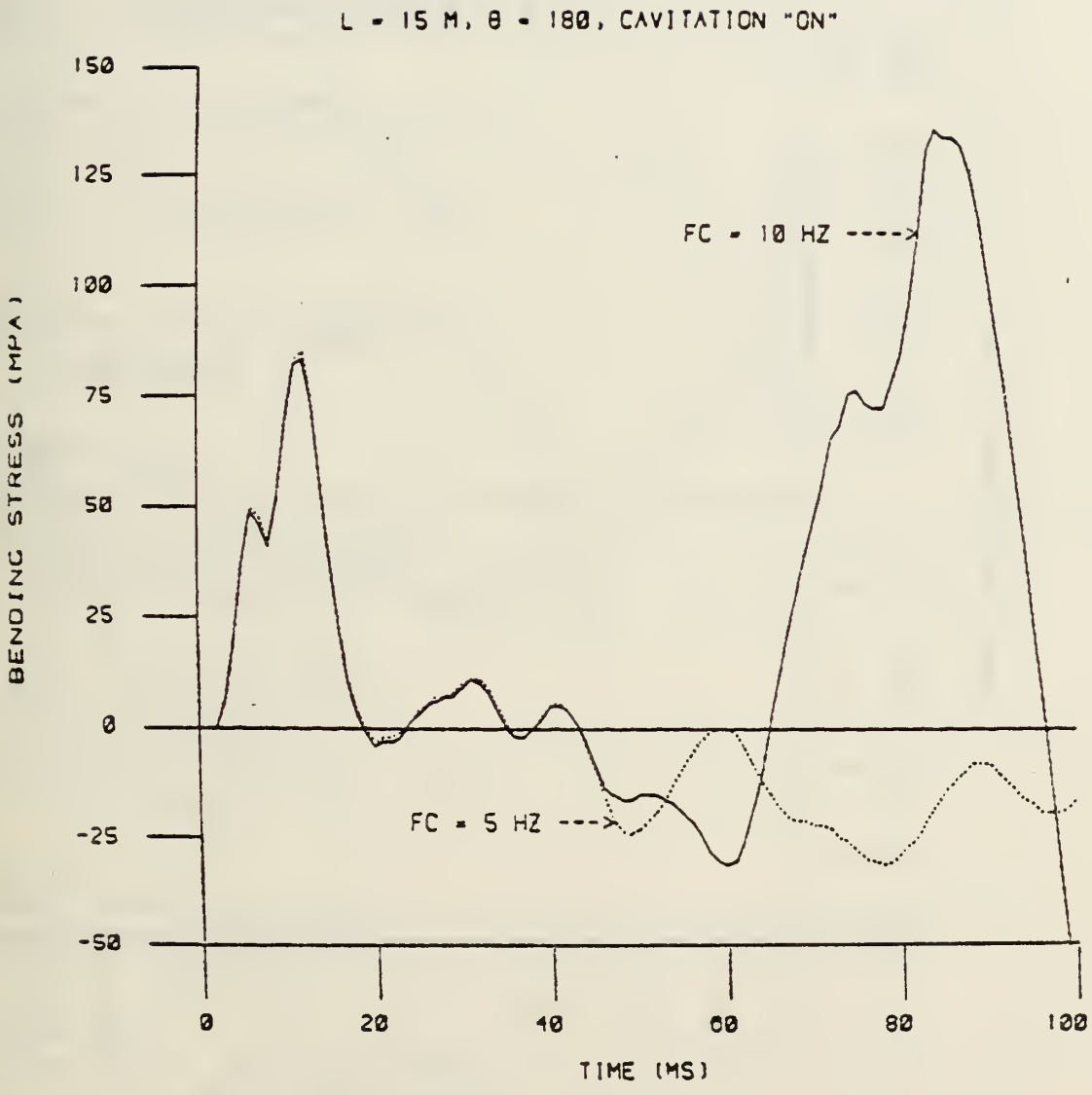

Fig. 12. Effect of suspension frequency on shell bending stress, L = 15 m.

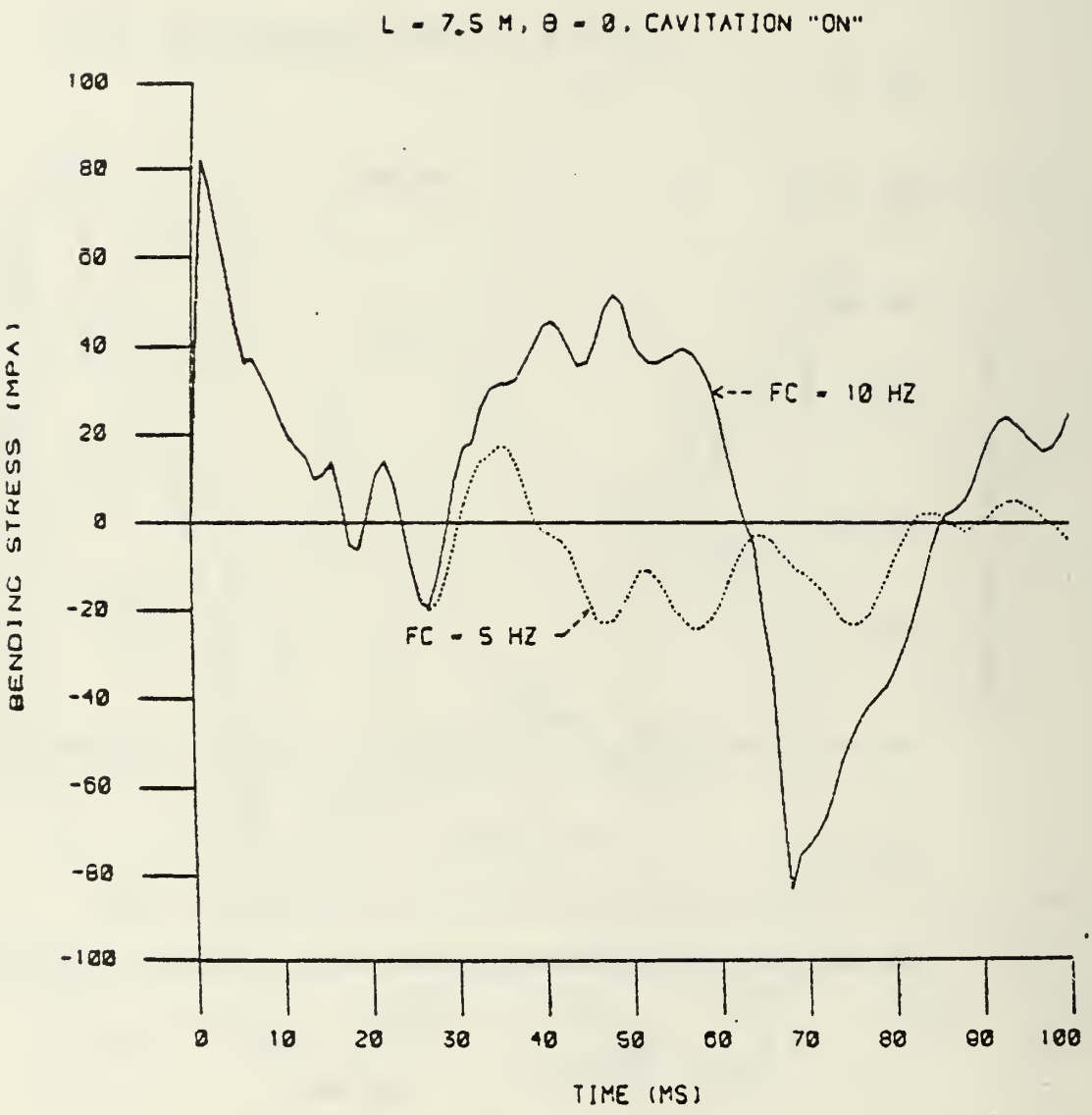

Fig. 13. Effect of suspension frequency on shell bending stress, L = 7.5 m.

INITIAL DISTRIBUTION LIST

		Copies
1.	Defense Technical Information Center Cameron Station Alexandria, Virginia 22314	2
2.	Research Administration, Code 012A Naval Postgraduate School Monterey, California 93940	1
3.	Professor R.E. Newton Mechanical Engineering Dept. Code 69Ne Naval Postgraduate School Monterey, California 93940	10
4.	Director Defense Nuclear Agency Washington, DC 20305 ATTN SPSS	10
5.	Commander Field Command Defense Nuclear Agency Kirtland Air Force Base Albuquerque, New Mexico 87117 ATTN Technical Library	1
6.	Chief - Field Command Defense Nuclear Agency Livermore Division P.O. Box 808, L-317 Livermore, California 94550 ATTN FCPRL	1
7.	Headquarters Naval Material Command Washington, DC 20360 ATTN MAT 08T-22	1
8.	Commander Naval Ocean Systems Center San Diego, California 92152 ATTN CODE 4471 Technical Library	1
9.	Superintendent Naval Postgraduate School Monterey, California 93940 ATTN CODE 0142 Library	2

Copies

10. Commander
Naval Sea Systems Command
Department of the Navy
Washington, DC 20362
ATTN SEA 322 J. Sullivan 1
ATTN SEA 09G53 Library 1

11. Commanding Officer
Naval Research Labratory
Washington, DC 20375
ATTN CODE 8440 G.O'Hara 1
ATTN CODE 8436 H. Huang 1

12. Commander
David W. Taylor Naval Ship Research and
Development Center
Bethesda, Maryland 20084
ATTN CODE 174 I. Hansen 1
ATTN CODE 1740.1 W. Sykes 1
ATTN CODE 1844 G. Everstine 1
ATTN CODE 1770.1 F. Costanzo 1
ATTN CODE 1740.5 B. Whang 1
ATTN CODE 172 R. Jones 1
ATTN CODE 1770.4 J. Gordon 1

13. Officer in Charge
Naval Construction Battalion Center
Civil Engineering Laboratory
Port Hueneme, California 93041
ATTN CODE 108A Library 1

14. Commander
Naval Surface Weapons Center
Dahlgren Laboratory
Dahlgren, Virginia 22448
ATTN Technical Library & Info Services Branch 1

15. Commanding
Naval Weapons Center
China Lake, California 93555
ATTN CODE 233 Technical Library 1

16. Commanding Officer
Naval Weapons Evaluation Facility
Kirtland Air Force Base
Albuquerque, New Mexico 87117
ATTN CODE 10 Technical Library 1

17. Officer in Charge
New London Laboratory
Naval Underwater Systems Center
New London, Connecticut 06320
ATTN CODE 401 J. Kalinowski 1

		Copies
18.	Office of Naval Research Department of the Navy Arlington, Virginia 22217 ATTN CODE 474 N. Perrone	1
19.	General Dynamics Corporation Electric Boat Division Eastern Point Road Groton, Connecticut 06340 ATTN M. PAKSTYS	1
20.	Lockheed Missiles and Space Company 3251 Hanover Street Palo Alto, California 94304 ATTN Technical Information Center ATTN T. Geers D/52-33 Bldg. 205	1 1
21.	Pacifica Technology P.O. Box 148 Del Mar, California 92014 ATTN J. Kent	1
22.	SRI International 333 Ravenswood Avenue Menlo Park, California 94025 ATTN G. Abrahamson ATTN A. Florence	1 1
23.	Weidlinger Associates 1801 Airline Boulevard Portsmouth, Virginia 23707 ATTN A. Misovec	1
24.	Weidlinger Associates 110 East 59th Street New York, NY 10022 ATTN M.L. Baron ATTN I.S. Sandler	1 1
25.	Columbia University Department of Civil Engineering S.W. Mudd Bldg. New York, NY 10027 ATTN F. DiMaggio	1